Transition-metal 13-atom clusters assessed with solid and surface-biased functionals

Maurício J. Piotrowski,[1,a)] Paulo Piquini,[1,b)] Mariana M. Odashima,[2,c)] and Juarez L. F. Da Silva[3,d)]
[1]*Departamento de Física, Universidade Federal de Santa Maria, Santa Maria, 97105-900, RS, Brazil*
[2]*Max-Planck Institut für Mikrostrukturphysik, Weinberg 2, D-06120 Halle, Germany*
[3]*Instituto de Física de São Carlos, Universidade de São Paulo, Caixa Postal 369, São Carlos, 13560-970 SP, Brazil*

(Received 20 January 2011; accepted 24 March 2011; published online 5 April 2011)

First-principles density-functional theory studies have reported open structures based on the formation of double simple-cubic (DSC) arrangements for Ru_{13}, Rh_{13}, Os_{13}, and Ir_{13}, which can be considered an unexpected result as those elements crystallize in compact bulk structures such as the face-centered cubic and hexagonal close-packed lattices. In this work, we investigated with the projected augmented wave method the dependence of the lowest-energy structure on the local and semilocal exchange-correlation (*xc*) energy functionals employed in density-functional theory. We found that the local-density approximation (LDA) and generalized-gradient formulations with different treatment of the electronic inhomogeneities (PBE, PBEsol, and AM05) confirm the DSC configuration as the lowest-energy structure for the studied TM_{13} clusters. A good agreement in the relative total energies are obtained even for structures with small energy differences, e.g., 0.10 eV. The employed *xc* functionals yield the same total magnetic moment for a given structure, i.e., the differences in the bond lengths do not affect the moments, which can be attributed to the atomic character of those clusters. Thus, at least for those systems, the differences among the LDA, PBE, PBEsol, and AM05 functionals are not large enough to yield qualitatively different results. © *2011 American Institute of Physics*. [doi:10.1063/1.3577999]

I. INTRODUCTION

Recently, well designed experimental studies have shown that subnanometer particles (clusters) composed of few metal atoms can play an important role in catalysis.[1–3] For example, aluminum cluster anion (Al_{17}^-) can produce H_2 from the addition of multiple water molecules;[2] platinum clusters (Pt_8) supported on Al_2O_3 are 40–100 times more active for oxidative dehydrogenation of propane than Pt/vanadium catalyst.[3] Thus, these results indicate that metal clusters can contribute to the development of industrial catalysis,[4] however, the challenges to obtain an atomistic understanding are complex. For example, a good cluster catalyst can abruptly turn down its performance upon a small change in the atomic structure, e.g., size change by adding or removing few atoms,[5,6] shape change,[7] ligands,[7] oxide support, which directly affects its reactivity. A large number of studies have been performed (see Refs. 8–10 and references therein), however, nowadays, the atomic structure of clusters and its dependence with the environment can still be considered as one of the main problems to be solved to obtain a better atomistic understanding in subnano catalysis.

Several experimental techniques, e.g., vibrational spectroscopy,[11] x-ray absorption spectroscopy,[12] photoelectron spectroscopy,[13,14] Stern–Gerlach like experiments,[15] have been used to characterize cluster properties, however, there are great difficulties to obtain the atomic structure (positions) of clusters directly.[8,9] Thus, theoretical approaches based on empirical pair-potentials,[16] semiempirical approaches such as the tight-binding method,[17,18] and first-principles calculations (see Refs. 10 and 19, and references therein) have been used to obtain the atomic structure of clusters, as well as its structure evolution with size.[20–31] However, even theoretical approaches face great challenges: (*i*) The number of local minimum configurations increase almost exponentially with the number of atoms.[9] (*ii*) Atomic pair-potentials combined with basin-hopping Monte Carlo (BHMC) (Refs. 16 and 32) algorithms are efficient to obtain the global minimum energy structures at low computational cost, however, pair-potentials have difficulties to provide a reliable description of transition-metal (TM) nanoparticles.[33,34] (*iii*) The combination of BHMC with density-functional theory (DFT) is still computationally very expensive and restricted for systems with few atoms.[35,36] (*iv*) Limitations in the local[37] and semilocal[38] exchange-correlation (*xc*) functionals in DFT, e.g., the self-interaction problem,[39] might affect particular properties as it does for bulk systems.[40–42]

Almost all the TM elements crystallize in compact structures, namely, face-centered cubic (fcc), body-centered cubic, and hexagonal close-packed (hcp).[43] Thus, it is

a)Electronic mail: mauriciomjp@gmail.com.
b)Electronic mail: paulo.piquini@ufsm.br.
c)Electronic mail: odashima@mpi-halle.de.
d)Author to whom correspondence should be addressed. Electronic mail: dasilva_juarez@yahoo.com.

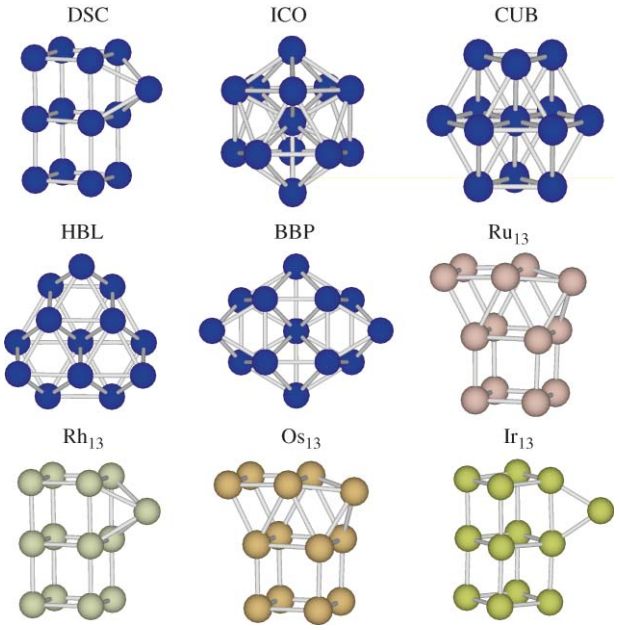

FIG. 1. Atomic model structures for TM_{13}: double simple-cubic (DSC), icosahedron (ICO), cuboctahedron (CUB), hexagonal bilayer (HBL), buckled biplanar (BBP), PBE lowest energy (LOW) for Ru_{13} (See Refs. 10, 19, 26, and 29), PBE LOW for Rh_{13} (See Refs. 10, 19, 26, 47, and 50), PBE LOW for Os_{13} (See Refs. 10, 19, and 26), PBE LOW for Ir_{13} (See Refs. 10, 19, and 26).

intuitively expected the formation of compact TM particles, e.g., cuboctahedron[9] (CUB), icosahedron[44] (ICO), Fig. 1, which have been confirmed by BHMC employing empirical Lennard-Jones[16] and Sutton–Chen[45,46] potentials. First-principles DFT calculations have confirmed the formation of ICO-like structures for several TM 13-atom clusters (TM_{13}), e.g., Sc, Ti, V, Cr, Mn, Fe, Y, Zr, Nb, Lu, Hf, Ta, and Hg, while slightly less compact structures, e.g., hexagonal bilayer (HBL), have been found for Co, Tc, and Re.[10,19,31,47–49]

However, recent calculations have identified the formation of open structures with simple-cubiclike shape for few systems, e.g., Ru_{13}, Rh_{13}, Os_{13}, and Ir_{13}.[10,19,26,29,47,50] Those open structures are composed by the stacking of two simple-cubic units (12 atoms), i.e., double simple-cubic (DSC), with the $13th$ atom added on one of the faces or corners of DSC, Fig. 1.[10,19,26,50] The effective coordination number (ECN) ranges from 3.30 to about 4.00,[10] which is smaller than the result obtained for ICO (ECN = 6.46).[10] Thus, based on structural analysis, the DSC-like configuration can be considered as an unexpected atomic configuration, since all the Ru, Rh, Os, and Ir systems crystallize in the fcc or hcp structures. Recently, Piotrowski *et al.*[10] reported a DFT study of the $3d$, $4d$, and $5d$ TM_{13} clusters, calculating about 50 configurations for Ru, Rh, Os, and Ir, including compact (ECN = 6.46), open (ECN = 3.00), and intermediate structures, but none of the calculated configurations could yield lower energy than DSC.

Among the known factors that can influence the quality of DFT calculations, one of the most important one is the approximation used to describe the *xc* functional. Although PBE is a successful functional, correcting a large part of the local-density approximation (LDA) (Ref. 37) overbinding, PBE commonly overestimates structural parameters by almost the same magnitude as the LDA functional underestimates. More recently, a new generation of generalized gradient approximations (GGA) were proposed with the aim to improve the structural properties of solids while preserving the computational costs of semilocal functionals. Among them, two were particularly designed to fulfil solid and surface constraints, namely, the Armiento–Mattsson[51] (AM05) formulation and the modified PBE for solids[52] (PBEsol). Both PBEsol and AM05 functionals are expected to provide a better description than LDA and PBE.[53,54] Although some of the limitations of the recent semilocal formulations have been discussed,[55,56] the surface-oriented character of these two functionals may be particularly interesting for the study of TM clusters. To our best knowledge, AM05 or PBEsol have not been assessed yet in TM clusters.

Therefore, in this work, we will investigate the performance of the PBEsol and AM05 functionals to describe the properties of the Ru_{13}, Rh_{13}, Os_{13}, and Ir_{13} clusters. For comparison, calculations will be also performed employing the LDA (Ref. 37) and PBE (Ref. 38) functionals. In order to obtain a good understanding of the performance of those functionals for clusters, and investigate the occurrence of the open DSC-like structures, we will calculate the relative total energies, total and local magnetic moments, average bond lengths, and average coordination numbers for TM_{13} clusters. Beyond the cluster calculations, we calculated the bulk properties of the respective systems.

II. THEORETICAL APPROACH AND COMPUTATIONAL DETAILS

Our calculations are based on spin-polarized DFT[57,58] calculations employing the LDA,[37] PBE,[38] PBEsol,[52] and AM05[51] to describe the *xc* energy functionals. The PBEsol has the same analytical form as in the PBE functional, but, two of its parameters are chosen to reproduce accurate values of the surface *xc* energy of jellium, and recover the second-order gradient expansion for exchange (relevant for the slowly varying density regime, such as valence electrons in densely packed solids). Differently from PBE and PBEsol, the AM05 functional was constructed from a subsystem functional approach[59] and specifically designed to treat systems with electronic surfaces, with an interpolation scheme that combines the Airy gas[60] and uniform electron gas.

The Kohn–Sham equations were solved using the all-electron projected augmented wave method,[61,62] as implemented in the Vienna *ab initio* simulation package (VASP).[63,64] For the LDA, PBE, and PBEsol calculations, the following plane-wave cutoff energies were employed: 230 (Ru), 271 (Rh), 228 (Os), and 210 eV (Ir). However, higher cutoff energies were required for the AM05 calculations, e.g., 460 (Ru), 542 (Rh), 456 (Os), and 420 eV (Ir), which is due to the convergence instability generated by the large number of gradients and the vacuum region,[65,66] i.e., the instabilities are not present for bulk calculations. Thus, at least for TM clusters, AM05 has a higher computational cost than PBE and PBEsol functionals.

The equilibrium volumes were obtained by minimizing the atomic forces and the stress tensor using the following

TABLE I. Equilibrium lattice constants, a_0, c_0, for the bulk Ru, Rh, Os, and Ir. The numbers in parentheses are the deviation (in %) with respect the experimental values (Ref. 43).

	Ru				Rh		Os				Ir	
	a_0 (Å)		c_0 (Å)		a_0 (Å)		a_0 (Å)		c_0 (Å)		a_0 (Å)	
LDA	2.69	(−0.74)	4.24	(−0.93)	3.77	(−0.79)	2.72	(−0.73)	4.29	(−0.69)	3.82	(−0.52)
PBE	2.73	(+0.74)	4.31	(+0.70)	3.85	(+1.32)	2.76	(+0.73)	4.35	(+0.69)	3.88	(+1.04)
PBEsol	2.70	(−0.37)	4.26	(−0.47)	3.80	(0.00)	2.74	(0.00)	4.31	(−0.23)	3.84	(0.00)
AM05	2.69	(−0.74)	4.25	(−0.70)	3.79	(−0.26)	2.72	(−0.73)	4.29	(−0.69)	3.83	(−0.26)
Expt.	2.71		4.28		3.80		2.74		4.32		3.84	

cutoff energies: 460 (Ru), 542 (Rh), 456 (Os), and 420 eV (Ir), for all functionals. All clusters were modeled using a cubic box of 17 Å. For the Brillouin zone integration, we employed a single **k**-point (Γ-point) for the clusters calculations, while for the bulk calculations, we employed **k**-mesh of $18 \times 18 \times 18$ for the bulk Rh and Ir in the fcc structure and $17 \times 17 \times 9$ for the bulk Ru and Os in the hcp structure. For all calculations, the equilibrium geometries are obtained when the forces on each atom are less than 0.010 eV/Å, with a total energy convergence criteria of 10^{-6} eV.

The cohesive energy of the bulk systems, E_{coh}, and the binding energy of the clusters, E_{b}, are defined as follows:

$$E_{\text{coh/b}} = E_{\text{tot}}^{\text{bulk/clusters}} - E_{\text{tot}}^{\text{freeatom}}, \quad (1)$$

where $E_{\text{tot}}^{\text{bulk/clusters}}$ is the total energy per atom for the bulk and cluster, respectively, while $E_{\text{tot}}^{\text{freeatom}}$ is the total energy of the free atom calculated using an orthorhombic structure.

III. RESULTS

A. Bulk properties

The lattice constants (a_0, c_0) and cohesive energies, E_{coh}, are summarized in Tables I and II, which are in excellent agreement with experimental values,[43] with errors smaller than 1.3% for all functionals. We obtained the expected trends for the LDA and PBE functionals,[38,41,54,67,68] i.e., LDA underestimates and PBE overestimates by similar magnitudes the lattice parameters. The AM05 slightly improves the lattice constants as compared with LDA and PBE but only for Rh and Ir, while PBEsol substantially improves a_0 and c_0 for all systems, which is expected as PBEsol was designed to improve the equilibrium volume of solids.[52]

The expected intermediate performance of PBEsol (14.61 − 21.18%) between the overbinding LDA (25.46 –33.14%) and underbinding PBE (−1.04 to −5.19%) in solids can be seen in Table II. PBE gives the best cohesive energies, i.e., smallest errors compared with experimental results,[43] while both AM05 (11.48–16.71%) and PBEsol overbind, however, with smaller errors compared with LDA. AM05 performs slightly better than PBEsol for those systems. Thus, our results can provide insights into the performance of AM05 to describe cohesive energies, which to our knowledge, have not been reported in literature.

TABLE II. Cohesive and binding energies, E_{coh} and E_{b} (in eV/atom), for the bulk and lowest energy TM_{13} clusters. For E_{coh}, the numbers in parentheses indicate the relative error in % with respect the experimental values, while for E_{b}, the numbers in parentheses indicate the magnitude of E_{b} with respect to E_{coh} in %.

	xc	Ru	Rh	Os	Ir
E_{coh}	LDA	−8.67(28.63)	−7.44(29.39)	−10.25(25.46)	−9.24(33.14)
	PBE	−6.66(−1.19)	−5.69(−1.04)	−8.32(−1.84)	−7.30(−5.19)
	PBEsol	−7.82(16.02)	−6.59(14.61)	−9.39(14.93)	−8.41(21.18)
	AM05	−7.52(11.57)	−6.41(11.48)	−9.24(13.10)	−8.10(16.71)
	Expt.	−6.74	−5.75	−8.17	−6.94
		Ru_{13}	Rh_{13}	Os_{13}	Ir_{13}
E_{b}	LDA	−5.86(67.59)	−5.02(67.47)	−6.96(67.90)	−6.48(70.13)
	PBE	−4.37(65.62)	−3.81(66.96)	−5.55(66.71)	−5.10(69.86)
	PBEsol	−5.18(66.24)	−4.37(66.31)	−6.25(66.56)	−5.82(69.20)
	AM05	−4.99(66.36)	−4.25(66.30)	−6.18(66.83)	−5.59(69.01)

B. Cluster TM_{13} properties

To perform this study, we selected the most representative structures reported so far for TM_{13},[9,10,19,26,50,69,70] which comprises five configurations, Fig. 1, namely, DSC,[10,19,26,50] ICO with point group I_h,[9,10,19,44] CUB with point group O_h,[9,10] hexagonal bilayer with point group C_{3v},[10,19,71] and the buckled-biplanar (BBP) with point group C_{2v},[10,69] structures. Furthermore, we selected the lowest energy (LOW) structures reported for Ru_{13}, Rh_{13}, Os_{13}, and Ir_{13},[10,19,26,29,47,50] which are indicated in Fig. 1 by their respective names. Although this particular set of atomic configurations is limited, it contains all representative structures observed for all $3d$, $4d$, and $5d$ TM_{13},[10,19] which includes compact, planar, and open structures.

1. Binding energies and relative total energies

The binding energies, E_b, are summarized in Table II and the relative total energies, ΔE_{tot}, are shown in Fig. 2 ($\Delta E_{\text{tot}}^{\text{config.}} = E_{\text{tot}}^{\text{config.}} - E_{\text{tot}}^{\text{ICO}}$). For all systems, we found that the absolute values of E_{b} follow: $E_{\text{b}}^{\text{LDA}} > E_{\text{b}}^{\text{PBEsol}} > E_{\text{b}}^{\text{AM05}} > E_{\text{b}}^{\text{PBE}}$, which is the same trend observed for the cohesive energy, Table II. For very large particles, it is known that E_{b} should approach the bulk cohesive energies,[9] and hence, it is interesting to compare the magnitude of E_{b} with respect to the value of E_{coh}. We found that E_{b} is, at average, 67.4% of the cohesive energy; for all systems, with values

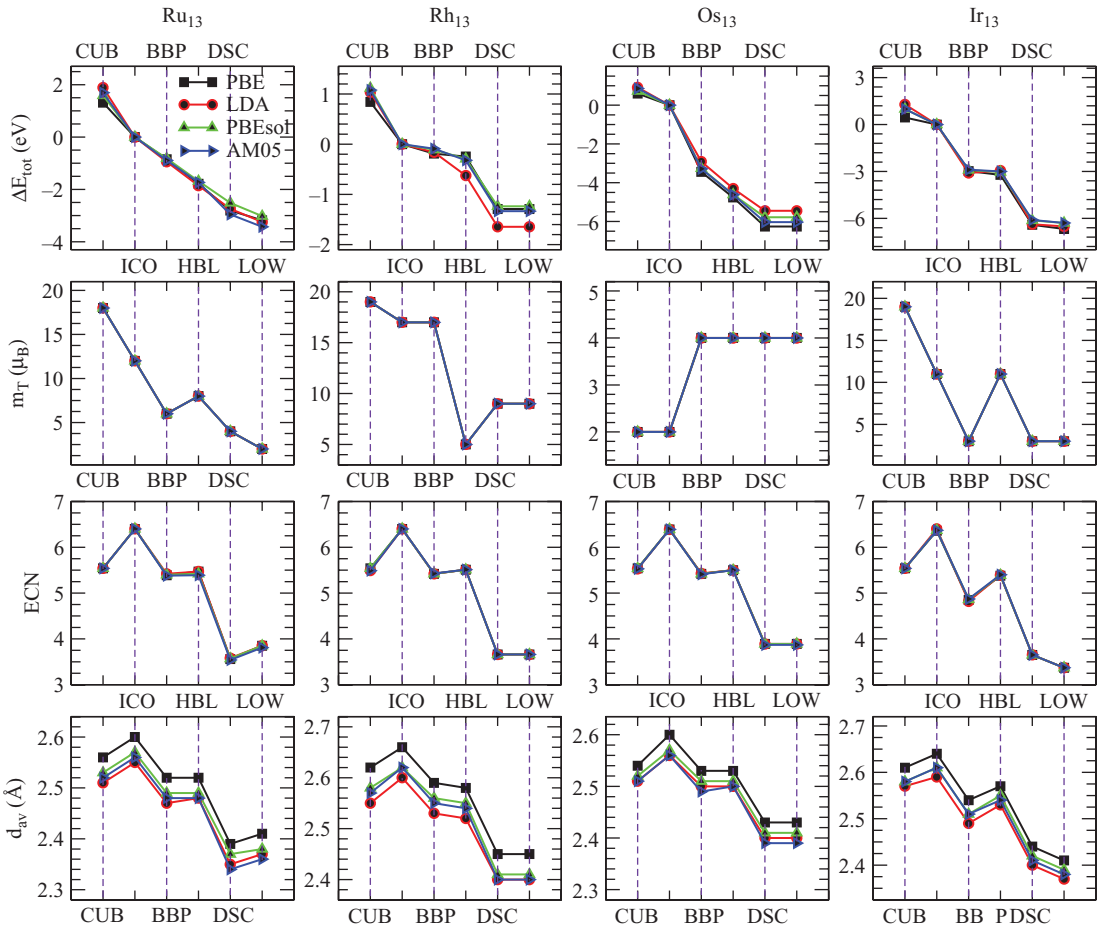

FIG. 2. Relative total energies, total magnetic moments, and average bond lengths for the Ru_{13}, Rh_{13}, Os_{13}, and Ir_{13} systems for the LDA, PBE, PBEsol, and AM05 functionals and ICO, CUB, BBP, HBL, DSC, and LOW structures, see Fig. 1. The relative energies are given with respect to the ICO configuration, i.e., $\Delta E_{\text{tot}} = E_{\text{tot}}^{\text{config.}} - E_{\text{tot}}^{\text{ICO}}$.

in the range of 65.62%–70.13%. Our results indicate that most of the relative errors are related with the description of the free-atoms, since all functionals yield a very similar proportion of the cluster to the bulk total energies. Using this factor (67.4%), we can estimate the *experimental binding energy* per atom of TM_{13} using the experimental bulk values,[43] which results in −4.54, −3.88, −5.51, and −4.68 eV for the Ru_{13}, Rh_{13}, Os_{13}, and Ir_{13}, respectively.

As far as the relative stability of the different cluster configurations are concerned, we found the following results: $\Delta E_{\text{tot}}^{\text{LOW}} \leq \Delta E_{\text{tot}}^{\text{DSC}} < \Delta E_{\text{tot}}^{\text{HBL}} < \Delta E_{\text{tot}}^{\text{BBP}} < \Delta E_{\text{tot}}^{\text{ICO}} < \Delta E_{\text{tot}}^{\text{CUB}}$. Thus, all *xc* functionals energetically favors the open DSC-like configuration for Ru_{13}, Rh_{13}, Os_{13}, and Ir_{13} instead of compact configurations, and hence, these results confirm previous studies.[10,19,49,72]

2. Structural analysis

In this work, we will employ the effective coordination concept,[73,74] which yields the average effective coordination number, ECN, and the average weighted bond lengths, d_{av}, Fig. 2.[10,34,75] It can be seen that all functionals yield the same ECN for a particular atomic configuration. We observed that the stability increases as the ECN decreases, and hence, the lowest energy DSC-like structures have the smallest ECN values. In contrast with ECN, the results for d_{av} show a clear dependence with the functionals, which is expected from our bulk calculations. PBE yields the largest average bond lengths, while LDA/AM05 yields the smallest ones, which is consistent with our bulk calculations. Our PBEsol values are in between the LDA/AM05 and PBE results. We would like to point out that there is no available experimental result for the average bond lengths.

The average bond lengths for the bulk, ICO, and LOW configurations are summarized in Table III. It can be clearly seen that the bond length of the ICO configuration is smaller than the bond length in the bulk phase by about 2.21–4.83% for all functionals and systems. For LOW, we observed even smaller bond lengths, e.g., from 9.93% to 12.22%, which is related with the smaller coordination of the LOW configurations, i.e., smaller coordination implies shorter bond lengths.[47]

3. Magnetic properties

It has been widely known that Ru, Rh, Os, and Ir are nonmagnetic at their ground state bulk structures,[43] which was confirmed by our calculations. However, the TM_{13} clusters show large total magnetic moments, Fig. 2, which is consistent with previous experimental[15,76] and theoretical[10,77]

TABLE III. Average bond length (in Å) for the bulk, ICO_{13}, and LOW_{13} clusters. The numbers in parentheses indicate the differences between clusters d_{av} and bulk d_{av} in %.

xc		Ru	Rh	Os	Ir
LDA	Bulk	2.66	2.67	2.69	2.70
	ICO_{13}	2.55(4.14)	2.60(2.62)	2.56(4.83)	2.59(4.07)
	LOW_{13}	2.37(10.90)	2.40(10.11)	2.40(10.78)	2.37(12.22)
PBE	Bulk	2.70	2.72	2.73	2.74
	ICO_{13}	2.60(3.70)	2.66(2.21)	2.60(4.76)	2.64(3.65)
	LOW_{13}	2.41(10.74)	2.45(9.93)	2.43(10.99)	2.41(12.04)
PBEsol	Bulk	2.67	2.69	2.70	2.71
	ICO_{13}	2.57(3.75)	2.62(2.60)	2.57(4.81)	2.61(3.69)
	LOW_{13}	2.38(10.86)	2.41(10.41)	2.41(10.74)	2.39(11.81)
AM05	Bulk	2.66	2.68	2.69	2.71
	ICO_{13}	2.56(3.76)	2.62(2.24)	2.56(4.83)	2.61(3.69)
	LOW_{13}	2.36(11.28)	2.40(10.45)	2.39(11.15)	2.38(12.18)

studies. We found that all functionals yield the same total magnetic moment, m_T, for a particular configuration and system, and hence, the differences in the functionals construction, in particular for AM05, do not play an important role in the magnitude of m_T, at least for these clusters. We would like to point out that the LDA calculations were performed using the flag `VOSKOWN = 1` in VASP, in order to run spin-polarized LDA using the accurate interpolation of Vosko, Wilk, and Nusair.[78] Otherwise, slightly smaller total magnetic moments are obtained.

As can be seen from Fig. 2, there is a clear dependence of m_T as a function of the cluster structure, however, there is no clear trend as a function of ECN. For Ru_{13}, Rh_{13}, and Ir_{13}, m_T is larger (smaller) for compact (open) structures such as the ICO and CUB (DSC), except for Os_{13}. The magnitude of m_T for the LOW structures is substantially smaller than for TM_{13} clusters of magnetic systems, e.g., Fe_{13}, Co_{13}, Ni_{13}.[31,48,79,80] Furthermore, we would like to mention that two different atomic configurations with similar total energies can have very different magnetic moments, e.g., for Ir_{13}, BBP, and HBL differ by about 0.20 eV for all functionals, while we obtained $m_T = 3.0\,\mu_B$ for BBP and $m_T = 11.0\,\mu_B$ for HBL. Thus, these results indicate that particular discrepancies among different DFT calculations employing local or semilocal functionals cannot be directly attributed to the functionals themselves, i.e., they are most likely related with differences in the atomic structures.

As previously reported in the literature,[10,29,47,50] DSC-like structures yield total magnetic moments for Ru_{13} ($m_T = 2\,\mu_B$) and Rh_{13} ($m_T = 9\,\mu_B$) in good agreement with experimental results obtained by Cox *et al.*, i.e., $< 3.77\,\mu_B$ and $6.24 \pm 1.69\,\mu_B$, respectively,[15,76] while the compact ICO structure yields $m_T = 12\,\mu_B$ for Ru_{13}^{ICO} and $17\,\mu_B$ for Rh_{13}^{ICO}. Thus, it looks that compact structures are unable to explain these experimental results. In order to investigate this problem further, we performed fixed magnetic moment PBE geometric optimizations for the DSC and ICO configurations for Rh_{13}. We found that configurations with $m_T = 3\,\mu_B$ (ferrimagnetic) and $9\,\mu_B$ (ferromagnetic) yield almost the same energy for DSC, while for ICO, we found similar energies for $m_T = 15$–$21\,\mu_B$ yield almost the same energy.

IV. SUMMARY

In this work, we reported DFT calculations within the local (LDA) and semilocal (PBE, PBEsol, AM05) functionals, of the binding energies, relative total energies, total magnetic moments, bond lengths, and coordination numbers for the Ru_{13}, Rh_{13}, Os_{13}, and Ir_{13} clusters. To the best of our knowledge, there are no systematic studies of the performance of the PBEsol and AM05 for TM_{13} clusters, and hence, this work provides important insights into the performance of these recent functionals. Although the four chosen functionals were constructed including different nonempirical constraints and paradigms see Sec. II, with different locality levels, we found that they provide essentially the same trends and results for all calculated properties. In particular, they yield the open DSC-like configuration as the lowest energy structures, confirming previous PBE results. However, from our understanding, these findings do not close the question about the unexpected open structures for TM_{13}. Our results only show that the differences in the local (LDA) and semilocal (PBE, PBEsol, AM05) formulations are not significant to lead to contrasting structural predictions for systems such as Ru_{13}, Rh_{13}, Os_{13}, and Ir_{13}. The same cannot hold for other systems such as bulk iron, for which the same functionals yield very different ground states phases. Therefore, we expected that more sophisticated formulations, which include nonlocal functionals or quantum Monte Carlo calculations can address the cluster atomic structure problem.

ACKNOWLEDGMENTS

M. Piotrowski and P. Piquini are thankful to the Brazilian financial agencies CNPq and CAPES, while Juarez L. F. Da Silva thanks São Paulo Science Foundation (FAPESP) for financial support.

[1] A. W. Castleman, Jr. and P. Jena, Proc. Natl. Acad. Sci. U.S.A. **103**, 10554 (2006).
[2] P. J. Roach, W. H. Woodward, A. W. Castlman, Jr., A. C. Reber, and S. N. Khanna, Science **323**, 492 (2009).
[3] S. Vajda, M. J. Pellin, J. P. Greeley, C. L. Marshall, L. A. Curtiss, G. A. Ballentine, J. W. Elam, S. Catillon-Mucherie, P. C. Redfern, F. Mehmood, and P. Zapol, Nature Mater. **8**, 213 (2009).
[4] F. C. Meunier, ACS Nano **2**, 2441 (2008).
[5] Z. Xu, F.-S. Xiao, S. K. Purnell, O. Alexeev, S. Kawi, S. E. Deutsch, and B. C. Gates, Nature (London) **372**, 346 (1994).
[6] Y. Sun, L. Zhuang, J. Lu, X. Hong, and P. Liu, J. Am. Chem. Soc. **129**, 15465 (2007).
[7] G. Schmid, Chem. Soc. Rev. **37**, 1909 (2008).
[8] J. A. Alonso, Chem. Rev. **100**, 637 (2000).
[9] F. Baletto and R. Ferrando, Rev. Mod. Phys. **77**, 371 (2005).
[10] M. J. Piotrowski, P. Piquini, and J. L.F. Da Silva, Phys. Rev. B **81**, 155446 (2010).
[11] P. Gruene, D. M. Rayner, B. Redlich, A. F.G. van der Meer, J. T. Lyon, G. Meijer, and A. Fielicke, Science **321**, 674 (2008).
[12] M. Reif, L. Glaser, M. Martins, and W. Wurth, Phys. Rev. B **72**, 155405 (2005).
[13] S.-R. Liu, H.-J. Zhai, and L.-S. Wang, Phys. Rev. B **64**, 153402 (2001).
[14] H. Häkkinen, B. Yoon, U. Landaman, X. Li, H.-J. Zhai, and L.-S. Wang, J. Phys. Chem. A **107**, 6168 (2003).

[15]A. J. Cox, J. G. Louderback, S. E. Apsel, and L. A. Bloomfield, Phys. Rev. B **49**, 12295 (1994).
[16]D. J. Wales and J. P. K. Doye, J. Phys. Chem. A **101**, 5111 (1997).
[17]B. Piveteau, M. C. Desjonquères, A. M. Oleś, and D. Spanjaard, Surf. Sci. **352**, 951 (1996).
[18]C. Barreteau, D. Spanjaard, and M. C. Desjonquères, Phys. Rev. B **58**, 9721 (1998).
[19]Y. Sun, M. Zhang, and R. Fournier, Phys. Rev. B **77**, 075435 (2008).
[20]P. Piquini, S. Canuto, and A. Fazzio, Nanostruct. Mater. **10**, 635 (1998).
[21]B. V. Reddy, S. K. Nayak, S. N. Khanna, B. K. Rao, and P. Jena, Phys. Rev. B **59**, 5214 (1999).
[22]V. Kumar and Y. Kawazoe, Phys. Rev. B **65**, 125403 (2002).
[23]W. Zhang, Q. Ge, and L. Wang, J. Chem. Phys. **118**, 5793 (2003).
[24]Y.-C. Bae, H. Osanai, V. Kumar, and Y. Kawazoe, Phys. Rev. B **70**, 195413 (2004).
[25]E. M. Fernádez, J. M. Soler, I. L. Garzón, and L. C. Balbás, Phys. Rev. B **70**, 165403 (2004).
[26]W. Zhang, L. Xiao, Y. Hirata, T. Pawluk, and L. Wang, Chem. Phys. Lett. **383**, 67 (2004).
[27]S.-Y. Wang, J.-Z. Yu, H. Mizuseki, J.-A. Yan, Y. Kawazoe, and C.-Y. Wang, J. Chem. Phys. **120**, 8463 (2004).
[28]H. K. Yuan, H. Chen, A. S. Ahmed, and J. F. Zhang, Phys. Rev. B **74**, 144434 (2006).
[29]S. Li, H. Li, J. Liu, X. Xue, Y. Tian, H. He, and Y. Jia, Phys. Rev. B **76**, 045410 (2007).
[30]V. Kumar and Y. Kawazoe, Phys. Rev. B **77**, 205418 (2008).
[31]R. Singh and P. Kroll, Phys. Rev. B **78**, 245404 (2008).
[32]H. G. Kim, S. K. Choi, and H. M. Lee, J. Chem. Phys. **128**, 144702 (2008).
[33]R. Fournier, J. Chem. Phys. **115**, 2165 (2001).
[34]J. L.F. Da Silva, H. G. Kim, M. J. Piotrowski, M. J. Prieto, and G. Tremiliosi-Filho, Phys. Rev. B **82**, 205424 (2010).
[35]S. Yoon and X. C. Zeng, Angew. Chem. Int. Ed. **44**, 1491 (2005).
[36]R. Gehrke and K. Reuter, Phys. Rev. B **79**, 085412 (2009).
[37]J. P. Perdew and Y. Wang, Phys. Rev. B **45**, 13244 (1992).
[38]J. P. Perdew, K. Burke, and M. Ernzerhof, Phys. Rev. Lett. **77**, 3865 (1996).
[39]A. Svane and O. Gunnarsson, Phys. Rev. Lett. **65**, 1148 (1990).
[40]M. Fuchs, J. L.F. Da Silva, C. Stampfl, J. Neugebauer, and M. Scheffler, Phys. Rev. B **65**, 245212 (2002).
[41]J. L.F. Da Silva, M. V. Ganduglia-Pirovano, J. Sauer, V. Bayer, and G. Kresse, Phys. Rev. B **75**, 045121 (2007).
[42]L. L. Wang and D. D. Johnson, J. Phys. Chem. B **109**, 23113 (2005).
[43]C. Kittel, *Introduction to Solid State Physics*, 7th ed. (Wiley, New York, 1996).
[44]A. L. Mackay, Acta Crystallogr. **15**, 916 (1962).
[45]A. P. Sutton and J. Chen, Philos. Mag. Lett. **61**, 139 (1990).
[46]J. P. K. Doye and D. J. Wales, New. J. Chem. **22**, 733 (1998).
[47]L.-L. Wang and D. D. Johnson, Phys. Rev. B **75**, 235405 (2007).
[48]C. D. Dong and X. G. Gong, Phys. Rev. B **78**, 020409(R) (2008).
[49]Y. Sun, R. Fournier, and M. Zhang, Phys. Rev. A **79**, 043202 (2009).
[50]Y.-C. Bae, V. Kumar, H. Osanai, and Y. Kawazoe, Phys. Rev. B **72**, 125427 (2005).
[51]R. Armiento and A. E. Mattsson, Phys. Rev. B **72**, 085108 (2005).
[52]J. P. Perdew, A. Ruzsinszky, G. I. Csonka, O. A. Vydrov, G. E. Scuseria, L. A. Constantin, X. L. Zhou, and K. Burke, Phys. Rev. Lett. **100**, 136406 (2008).
[53]G. I. Csonka, J. P. Perdew, A. Ruzsinszky, P. H. T. Philipsen, S. Lebégue, J. Paier, O. A. Vydrov, and J. G. Ángyán, Phys. Rev. B **79**, 155107 (2009).
[54]P. Haas, F. Tran, and P. Blaha, Phys. Rev. B **79**, 085104 (2009).
[55]J. P. Perdew, A. Ruzsinszky, G. I. Csonka, L. A. Constantin, and J. Sun, Phys. Rev. Lett. **103**, 026403 (2009).
[56]M. Kodera, T. Shishidou, and T. Oguchi, J. Phys. Soc. Jpn. **79**, 074713 (2010).
[57]P. Hohenberg and W. Kohn, Phys. Rev. **136**, B864 (1964).
[58]W. Kohn and L. J. Sham, Phys. Rev. **140**, A1133 (1965).
[59]W. Kohn and A. E. Mattsson, Phys. Rev. Lett. **81**, 3487 (1998).
[60]L. Vitos, B. Johansson, J. Kollá, and H. L. Skriver, Appl. Phys. B **62**, 10046 (2000).
[61]P. E. Blöchl, Phys. Rev. B **50**, 17953 (1994).
[62]G. Kresse and D. Joubert, Phys. Rev. B **59**, 1758 (1999).
[63]G. Kresse and J. Hafner, Phys. Rev. B **48**, 13115 (1993).
[64]G. Kresse and J. Furthmüller, Phys. Rev. B **54**, 11169 (1996).
[65]A. E. Mattsson, R. Armiento, J. Paier, G. Kresse, J. M. Wills, and T. R. Mattsson, J. Chem. Phys. **128**, 084714 (2008).
[66]A. E. Mattsson and R. Armiento, Phys. Rev. B **79**, 155101 (2009).
[67]A. Khein, D. J. Singh, and C. J. Umrigar, Phys. Rev. B **51**, 4105 (1995).
[68]M. Fuchs and M. Scheffler, Comput. Phys. Commun. **119**, 67 (1999).
[69]C. M. Chang and M. Y. Chou, Phys. Rev. Lett. **93**, 133401 (2004).
[70]J. P. Chou, H. Y. T. Chen, C. R. Hsing, C. M. Chang, C. Cheng, and C. M. Wei, Phys. Rev. B **80**, 165412 (2009).
[71]T. Futschek, M. Marsman, and J. Hafner, J. Phys.: Condens. Matter **17**, 5927 (2005).
[72]M. Zhang and R. Fournier, Phys. Rev. A **79**, 043203 (2009).
[73]R. Hoppe, Angew. Chem., Int. Ed. **9**, 25 (1970).
[74]R. Hoppe, Z. Kristallogr. **150**, 23 (1979).
[75]J. L. F. Da Silva, A. Walsh, and S.-H. Wei, Phys. Rev. B **80**, 214118 (2009).
[76]A. J. Cox, J. G. Louderback, and L. A. Bloomfield, Phys. Rev. Lett. **71**, 923 (1993).
[77]B. V. Reddy, S. N. Khanna, and B. I. Dunlap, Phys. Rev. Lett. **70**, 3323 (1993).
[78]S. H. Vosko, L. Wilk, and M. Nusair, Can. J. Phys. **58**, 1200 (1980).
[79]B. I. Dunlap, Phys. Rev. A **41**, 5691 (1990).
[80]F. Aguilera-Granja, J. M. Montejano-Carrizalez, and R. A. Guirado-López, Phys. Rev. B **73**, 115422 (2006).